

Investigation of routes and funnels in protein folding by free energy functional methods

Steven S. Plotkin and José N. Onuchic

Department of Physics, University of California, San Diego

October 27, 2018

ABSTRACT We use a free energy functional theory to elucidate general properties of heterogeneously ordering, fast folding proteins, and we test our conclusions with lattice simulations. We find that both structural and energetic heterogeneity can lower the free energy barrier to folding. Correlating stronger contact energies with entropically likely contacts of a given native structure lowers the barrier, and anticorrelating the energies has the reverse effect. Designing in relatively mild energetic heterogeneity can eliminate the barrier completely at the transition temperature. Sequences with native energies tuned to fold uniformly, as well as sequences tuned to fold by a single or a few routes, are rare. Sequences with weak native energetic heterogeneity are more common; their folding kinetics is more strongly determined by properties of the native structure. Sequences with different distributions of stability throughout the protein may still be good folders to the same structure. A measure of folding route narrowness is introduced which correlates with rate, and which can give information about the intrinsic biases in ordering due to native topology. This theoretical framework allows us to systematically investigate the coupled effects of energy and topology in protein folding, and to interpret recent experiments which investigate these effects.

The energy landscape has been a central paradigm in understanding the physical principles behind the self-organization of biological molecules [1–4]. A central feature of landscapes of biomolecules which has emerged is that the process of evolution, in selecting for sequences that fold reliably to a stable conformation within a biologically relevant time, induces a new energy scale into the landscape [5–7]. In addition to the ruggedness energy scale already present in heteropolymers, it now has the overall topography of a funnel [2, 8–10]. A sequence with a funneled landscape has a low energy native state occupied with large Boltzmann weight at temperatures high enough that folding kinetics is not dominated by slow escape from individual traps.

As an undesigned heteropolymer with a random, un-evolved sequence is cooled, it becomes trapped into one of many structurally different low energy states, similar to the phase transitions seen in spin glasses, glasses, and rubber. The low temperature states typically look like a snapshot of the high temperature collapsed states, but have dramatically slower dynamics. On the other hand, when a designed heteropolymer or protein is cooled, it reliably and quickly finds the dominant low energy structure(s) corresponding to the native state, in a manner similar to the phase transition from the gas or liquid to the crystal state. As in crystals, the low temperature states typically have a lower symmetry group than the many high temperature states [11]. Connections have been made between native structural symmetry and robustness to mutations of proteins [11–13]. Funnel topographies are maximized in atomic clusters when highly symmetric arrangements of the atoms are possible, as in van der Waals clusters with “magic numbers” [14, 15], and similar arguments have been applied to proteins [11], where funneled landscapes are directly connected to mutational robustness [16].

It is appealing to make the connection between symmetry and designability of native structures to the actual kinetics of the folding process, arguing that symmetry or uniformity *in ordering* the protein maximizes the number of folding routes and thus the ease of finding a candidate folding nucleus, thus maximizing the folding rate. Explicit signatures of multiple folding routes as predicted by the funnel theory [17, 18] have been seen in simulations of well-designed proteins [8, 19–23] as well as experiments on several small globular proteins [24–26]. However these folding routes are not necessarily equivalent. There is an accumulating body of experimental [27–31] and simulation [22, 32–42] evidence which show varying degrees of heterogeneity in the ordering process. These data refine the funnel picture by focusing on which parts of the protein most effectively contribute to ordering, and on the effects of native topology and na-

tive energy distribution on rates and stability. The ensemble of foldable sequences with a given ratio of $T_F/T_G > 1$ has a wide distribution of mean first passage times [17, 33, 43], indicating that several other properties of the sequence and structure contribute to folding thermodynamics and kinetics. These include topological properties of the native structure [11, 44–50] (e.g. mean loop length $\bar{\ell}$, dispersion in loop length $\delta\ell$, and kinetic accessibility of the native structure), the distribution over contacts of total native energy in the protein, and the coupling of contact energetics with native topology.

In this paper we integrate the above sundry observations into a theory which explicitly accounts for native heterogeneity, structural and energetic, in the funnel picture. We introduce a simple field theory with a non-uniform order parameter to study fluctuations away from uniform ordering, through free energy functional methods introduced earlier by Wolynes and collaborators [36, 48].¹ The theory is in agreement with simulations also performed in this paper. We organize the paper as follows. First we outline the calculation and results. Next we derive and use an approximate free energy functional which captures the essence of the problem. Then we conclude and suggest future research, leaving technical aspects of the derivation for the methods section.

OUTLINE. The free energy functional description in principle allows for a fairly complete understanding of the folding process for a particular sequence; this includes effects due to the three dimensional topological native structure, possible misfolded traps, and heterogeneity among the energies of native contacts. We model a well-designed, minimally frustrated protein with an approximate functional, but many of the results we obtain are quite general. We find that for a well-designed protein, gains in loop entropy and/or core energy always dominate over losses in route entropy, so the thermodynamic folding barrier is always reduced by any preferential ordering in the protein.²

¹ We treat only native couplings in detail, accounting for non-native interactions as a uniform background field. Additionally, the correlation between contacts (i, j) is a function only of the overall order Q in our theory. This is analogous to the Hartree approximation in the one-electron theory of solids [51] where electrons mutually interact only through an averaged field; extensions of our theory to include correlation mediated by native structure may be examined within the density-functional framework, and are a topic of future research. On the other hand, tests of the theory by simulation (fig. (1)) produce qualitatively the same results, so the conclusions are not effected by including correlations to any order.

² Folding heterogeneity effects the free energy in three ways: 1.) The number of folding routes to the native state decreases; this effect increases the folding barrier, 2.) The conformational entropy of polymer loops increases, since native cores

However as long as ordering heterogeneity is not too large, there are still many folding routes to the native structure, and the funnel picture is valid. When there are very few routes to the native state due to large preferential ordering, folding is slow and multi-exponential at temperatures where the native structure is stable. In this scenario the rate is governed by the kinetic traps along the path induced, rather than the putative thermodynamic barrier which is absent. Several physically motivated arguments giving the above results are described in the supplementary material.

To analyze the effects of native energetic as well as structural heterogeneity on folding, we coarsely describe the native structure through its distributions of native contact energies $\{\epsilon_i\}$ and native loop lengths $\{\ell_i\}$. Here ϵ_i is the solvent averaged effective energy of contact i , and ℓ_i is the sequence length pinched off by contact i . The labeling index i runs from 1 to M , where $M = zN$ is the total number of contacts, N is the length of the polymer, z the number of contacts per residue. In the spirit of density functional theory of fluids [52] we introduce a coarse-grained free energy functional $F(\{Q_i(Q)\} | \{\epsilon_i\}, \{\ell_i\})$ approximating the physics of secondary (as e.g. along a helix) and tertiary (non-local) contacts in ordering. Q is defined as the overall fraction of native contacts made, used here to *stratify* the configurations with given similarity to the native state, since this partitioning results in a funnel topography of the energy landscape for designed sequences [9, 10]. The fraction of time contact i is made in the sub-ensemble of states at Q is $Q_i(Q)$. From a knowledge of this functional all relevant thermodynamic functions can in general be calculated such as transition state entropies and energies, barrier heights, and surface tensions. Moreover, derivatives of the functional give the equilibrium distribution and correlation functions describing the microscopic structure of the inhomogeneous system, as we see below.

Given all the contact energies $\{\epsilon_i\}$ and loop lengths $\{\ell_i\}$ for a protein, the thermal distribution of contact probabilities $\{Q_i(Q)\}$ is found by minimizing the free energy functional $F(\{Q_i(Q)\} | \{\epsilon_i\}, \{\ell_i\})$ subject to the constraint that the average probability is Q , i.e. $\sum_i Q_i = MQ$ (Q parameterizes the values of the Q_i 's)³ Since in the model the probability of a con-

with larger halo entropies are more strongly weighted. This decreases the folding barrier 3.) Making likely contacts stronger in energy lowers the thermal energy of partially native structures; this decreases the folding barrier.

³ This procedure is analogous to finding the most probable distribution of occupation numbers, and thus the thermodynamics, by maximizing the microcanonical entropy for a sys-

tact to be formed is a function of its energy and loop length, we can next consider the minimized free energy as a function of the contact energies for a *given* native topology: $F(\{\epsilon_i\}|\{\ell_i\})$. Then we can seek the special distribution of contact energies $\{\epsilon_i^*(\ell_i)\}$ that minimizes or maximizes the thermodynamic folding barrier to a particular structure by finding the extremum of $F^\dagger(\{\epsilon_i\}|\{\ell_i\})$ with respect to the contact energies ϵ_i , subject to the constraint of fixed native energy, $\sum_i \epsilon_i = M\bar{\epsilon} = E_N$. This distribution when substituted into the free energy gives in principle the extremum free energy barrier as a function of native structure $F^\dagger(\{\ell_i\})$, which might then be optimized for the fastest/slowest folding structure and its corresponding barrier. We found that in fact the only distribution of energies for which the free energy was an extremum is in fact the distribution which *maximizes* the barrier by tuning all the contact probabilities to the same value.

METHODS. We derive an approximate free energy functional, which takes account for ordering heterogeneity, starting from a contact Hamiltonian $\mathcal{H}(\{\Delta_{\alpha\beta}\}|\{\Delta_{\alpha\beta}^N\})$ of the form

$$\mathcal{H} = \sum_{\alpha < \beta} [\epsilon_{\alpha\beta}^N \Delta_{\alpha\beta} \Delta_{\alpha\beta}^N + \epsilon_{\alpha\beta} \Delta_{\alpha\beta} (1 - \Delta_{\alpha\beta}^N)] \quad (1)$$

Here the double sum is over residue indices, $\Delta_{\alpha\beta} = 1$ (0) if residues α and β (do not) contact each other, $\Delta_{\alpha\beta}^N = 1$ (0) if these residues (do not) contact each other in the native configuration. The sum over native energies $\epsilon_{\alpha\beta}^N$ and non-native energies $\epsilon_{\alpha\beta}$ gives the energy for a particular configuration.⁴ To obtain the thermodynamics we proceed by obtaining the distribution of state energies in the microcanonical ensemble by averaging non-native interactions over a Gaussian distribution of variance b^2 : $P(E|E_N, \{\Delta_{\alpha\beta} \Delta_{\alpha\beta}^N\}) = \langle \delta[E - \mathcal{H}\{\Delta_{\alpha\beta}\}] \delta[E_N - \mathcal{H}\{\Delta_{\alpha\beta}^N\}] \rangle_{n-nat}$.⁵ The averaging results in a Gaussian distribution having mean $\sum_i \epsilon_i Q_i$ and variance $Mb^2(1 - Q)$, where $Q_i \equiv \Delta_{\alpha\beta} \Delta_{\alpha\beta}^N$ counts native contacts present in the configuration state inside the stratum Q . From this distribution the log density of states is obtained in terms of the configurational entropy of stratum Q , $S(\{Q_i\}|Q)$, and the free energy functional $F(\{Q_i\}|Q)$ obtained by performing

tem of particles obeying a given occupation statistics - here the effective particles (the contacts) obey Fermi-Dirac statistics, c.f. eq. (7).

⁴A similar derivation of the free energy for a uniform order parameter Q was calculated in ref. [10].

⁵This approach assumes minimal frustration, in that native heterogeneity is explicitly retained and non-native heterogeneity is averaged over; phenomena specific to a particular set of non-native energies, e.g. “off-pathway” intermediates, are smoothed over in this procedure.

the usual Legendre transform to the canonical ensemble (c.f. eq (4)).⁶

We express the free energy in terms of an arbitrary distribution of contact probabilities - the distribution of $\{Q_i\}$ that minimizes $F(\{Q_i\}|Q)$ is the (most probable) thermal distribution.⁷ For the ensemble of configurations at Q , we define the entropy that corresponds to the multiplicity of contact patterns as $\mathcal{S}_{\text{ROUTE}}(\{Q_i\}|Q)$ (> 0), and the configurational entropy lost from the coil state to induce a contact pattern $\{Q_i\}$ as $\mathcal{S}_{\text{BOND}}(\{Q_i\}|\{\ell_i\}, Q)$ (< 0). We make no capillarity or spinodal assumption, and treat the route entropy as the entropy of a binary fluid mixture [10, 53], modified by a prefactor $\lambda(Q) \equiv 1 - Q^\alpha$, which measures the number of combinatoric states reduced by chain topology: residues connected by a chain have less mixing entropy than if they were free⁸:

$$\mathcal{S}_{\text{ROUTE}} = \lambda(Q) \sum_{i=1}^M [-Q_i \ln Q_i - (1 - Q_i) \ln (1 - Q_i)]. \quad (2)$$

We introduce a measure of “routing” $\mathcal{R}(Q)$ by expanding the entropy to lowest order⁹: $\mathcal{S}_{\text{ROUTE}}(\{Q_i\}) \cong \mathcal{S}_{\text{ROUTE}}^{\text{MAX}} - \lambda \mathcal{R}(Q)/2$, where we have defined $\mathcal{R}(Q)$ by $\mathcal{R}(Q) = \langle \delta Q^2 \rangle / \langle \delta Q^2 \rangle_{\text{MAX}}$, which is the variance of contact probabilities normalized by the maximal variance,¹⁰ In the limit $\mathcal{R}(Q) = 0$ the uniformly ordering system has the maximal route entropy. When $Q_i = 0$ or 1 only, $\mathcal{R}(Q) = 1$, $\mathcal{S}_{\text{ROUTE}} = 0$, and only one route to the native state is allowed.¹¹

In the supplementary material we derive a form

⁶Note that in eq. (4) we explicitly include the thermal trace over configurations at overall order Q .

⁷In the contact representation, the averaged bond occupation probabilities $Q_i = \langle Q_i \rangle_{\text{TH}}$ are analogous to the averaged number density operator in an inhomogeneous fluid: $\langle n(\mathbf{x}) \rangle_{\text{TH}} = \langle \sum_i \delta(\mathbf{x}_i - \mathbf{x}) \rangle_{\text{TH}}$.

⁸The value $\alpha = 1.37$ gives the best fit to the lattice 27-mer data for the route entropy, while $\alpha \cong 1.0$ best fits the 27-mer free energy function. We generally use $\alpha \cong 1.0$ since the 27-mer is small - for larger systems α is smaller: more polymer is buried and thus more strongly constrained by surrounding contacts.

⁹We avoid the word “pathway” since several definitions exist in the literature; here a single route is unambiguously defined through the limit $\mathcal{S}_{\text{ROUTE}} \rightarrow 0$.

¹⁰That is, if MQ contacts were made with probability 1 and $M - MQ$ contacts were made with probability 0, then $\langle (Q_i - Q)^2 \rangle_{\text{MAX}} = (1/M)(MQ(1 - Q)^2 + (M - MQ)Q^2) = Q(1 - Q)$. Thus $\mathcal{R}(Q)$ is between 0 and 1.

¹¹That is, since all Q_i are only zero or one at any degree of nativeness, each successive bond added must always be the same one, so folding is then a random-walk on the potential defined by that *single* route (there is still chain entropy present). $\mathcal{R}(Q)$ is in the spirit of a Debye-Waller factor applied to folding routes.

for the configurational entropy loss to fold to a given topological structure by accounting for the distribution of entropy losses to form bonds or contacts due to the distribution of sequence lengths in that structure. We let the effective sequence (loop) length between residues i and j , $\ell_{\text{EFF}}(|i-j|, Q)$ be a function of Q (this is a mean field approximation), and we take the entropy loss to close this loop to be of the Flory form $\sim (3/2) \ln(a/\ell_{\text{EFF}})$. The requirement that the entropy be a state function restricts the possible functional form of the effective loop length. The result of the derivation for the contact entropy loss to form state $\{Q_i\}$ is

$$\mathcal{S}_{\text{BOND}} = -(3/2)M (\langle \delta Q \delta \ln \ell \rangle + S_{\text{MF}}(Q, \bar{\ell})) \quad (3)$$

where $\langle \delta Q \delta \ln \ell \rangle = (1/M) \sum_i (Q_i - Q)(\ln \ell_i - \overline{\ln \ell})$ is the correlation between the fluctuations in contact probability and log loop length, and $S_{\text{MF}}(Q, \bar{\ell})$ is the mean-field bond entropy loss (described in the supplement), and is a function only of Q and the mean loop length $\bar{\ell}$. By eq. (3) the entropy is *raised* above that of a symmetrically ordering system when shorter ranged contacts have higher probability to be formed; this effect lowers the barrier. Eqs (4), (2), and (3) together give expression (6) for the free energy $F(\{Q_i(Q)\} | \{\epsilon_i\}, \{\ell_i\})$ of a well-designed protein that orders heterogeneously.

The lattice protein used in fig 1 to check the theory is a chain of 27 monomers constrained to the vertices of a 3-D cubic lattice. Details of the model and its behavior can be found in [8, 19, 21, 32, 42, 43]. Monomers have non-bonded contact interactions with a Gō potential (native interactions only).¹² Coupling energies were chosen for row 1 of fig 1 by first running a simulated annealing algorithm to find the set $\{\epsilon_i^*\}$ that makes all the $Q_i(\{\epsilon_i^*\}) = Q^*$ at the barrier peak. Energies are always constrained to sum to a fixed total native energy: $\sum_i \epsilon_i = M\bar{\epsilon}$. Then energies were relaxed by letting $\epsilon_i = \epsilon_i^* + \alpha(\bar{\epsilon}_i - \epsilon_i^*)$. The values $\alpha = 1, 1.35, 2.05$ were used in rows 2, 3, and 4 respectively.

FREE ENERGY FUNCTIONAL. By averaging a contact Hamiltonian over non-native interactions, we can derive an approximate free energy functional for a well-designed protein (See the methods section). We analyze here heterogeneity in minimally frustrated sequences, where the roughness energy scale b is smaller than the stability gap $\bar{\epsilon}$. The general

form of the free energy functional is

$$F = \left\langle \sum_{i=1}^M [\epsilon_i Q_i - TS(\{Q_i\}|Q)] \right\rangle'_{\text{THERM}} - \frac{Mb^2}{2T} (1 - Q) \quad (4)$$

where $Q_i = (0, 1)$ counts native contacts in a configurational state (so the sum on $\epsilon_i Q_i$ gives the states energy), summing $S(\{Q_i\}|Q)$ gives the states configurational entropy, and then this is thermally averaged over all states restricted to have MQ contacts. The second term accounts for low energy non-native traps.

The study of the configurational entropy is a fascinating but complicated problem detailed in the methods section. In summary this entropy functional generalizes the Flory mean-field result [53, 54] to account for the topological heterogeneity inherent in the native structure and a finite average return length for that structure (contact order [47]), as well as to account for the number of folding routes to the native structure. The amount of route diversity or narrowness in folding can be quantified in terms of the relative fluctuations of contact formation $\delta Q = Q_i(Q) - Q$:

$$\mathcal{R}(Q) = \langle \delta Q^2 \rangle / \langle \delta Q^2 \rangle_{\text{MAX}} \quad , \quad (5)$$

which is useful for our analysis below. Our resulting analytic expression for the free energy of a protein that folds heterogeneously is¹³.

$$\frac{F}{M} \cong \frac{F_{\text{MF}}^o}{M} + \overline{\delta Q \delta \epsilon} + \frac{\lambda T}{2} \frac{\overline{\delta Q^2}}{Q(1-Q)} + \frac{3}{2} \overline{\delta Q \delta \ln \ell} \quad (6)$$

Here $F_{\text{MF}}^o(Q)$ is the uniform-field free energy function (similar to that obtained previously in [10]). The free energy functional is approximate in that it results from an integration over a local free energy density whose only information about the surrounding medium is through the average field present (Q), $F = \sum_i f_i(Q_i, Q)$. Cooperative entropic effects due to local correlations [48, 55] between contacts would be an important extension of the model, and have been treated elsewhere in similar models [48]. Inspection of eq. (6) shows that as heterogeneity increases, the effect on the barrier is a competition between energetic and polymer entropy gains (2nd and 4th terms) and route entropy losses (3rd term) as described above.

Minimizing the free energy (6) at fixed Q , $\delta(F + \mu \sum_j Q_j) = 0$, gives a Fermi distribution for the most

¹²Corner, crankshaft, and end moves are allowed. Free energies and contact probabilities are obtained by equilibrium monte-carlo sampling using the histogram method [43]. Sampling error is $< 5\%$.

¹³We have expanded the route entropy eq. (2) to second order in this expression for clarity; in deriving the results of the theory the full expression is used.

probable bond occupation probabilities $\{Q_i^*\}$ for a given $\{\epsilon_i\}$ and $\{\ell_i\}$:

$$Q_i^*(Q) = 1 / (1 + \exp[(\mu' + \epsilon_i - Ts_i) / \lambda T]) \quad (7)$$

where the Lagrange multiplier $\mu' \sim -(1/M)\partial F/\partial Q$ is related to the effective force on the potential $F(Q)$. Positive second variation of F indicates the extremum is in fact a minimum.

OPTIMIZING RATES, STABILITY, AND ENTROPY We now consider the effects on the free energy when the native interactions between residues are changed in a controlled manner. The theory predicts a barrier at the transition temperature of a few $k_B T$, in general agreement with experiments on small, single-domain proteins. The barrier height is fairly small compared to the total thermal energy of the system, reflecting the exchange of entropy for energy as the protein folds. However the barrier height can vary significantly depending on which parts of the protein are more stable in their local native structure. At uniform stability we find the largest barrier (for a given total native energy): about twice as large as the barrier when stability is governed purely by the three-dimensional native structure, i.e. when all interaction energies are equal. Increasing heterogeneity, by energetically favoring regions of the protein which are already entropically likely to order, systematically decreases the barrier, and in fact can eliminate the barrier entirely if the heterogeneity is large enough. See figure 1.

We seek to relax the values of $\{\epsilon_j\}$ at fixed native energy $E_N = \sum_j \epsilon_j$ to the distribution $\{\epsilon_i^* \mid \{\ell_j\}\}$ that extremizes the free energy barrier, by finding the solution of $\sum_i [\delta F^\ddagger / \delta \epsilon_i - p] \delta \epsilon_i = 0$ for arbitrary and independent variations $\delta \epsilon_i$ in the energies. It can be shown that $\delta F / \delta \epsilon_i = \partial F / \partial \epsilon_i + \mu(\delta / \delta \epsilon_i) \sum_j Q_j$, however the second term is zero since $\delta Q / \delta \epsilon_i = 0$, so by eq. (4) $\delta F / \delta \epsilon_i = Q_i$: the contact probability plays the role of the local density, and the perturbation $\delta \epsilon_i$ the role of an external field, as in liquid state theory. At the extremum all contact probabilities are equal: $Q_i = p = Q^\ddagger$, which in our model means that longer loops have lower (stronger) energies: $\delta \epsilon_i = T \delta s_i = -(3/2)T \delta \ln \ell_i$; there is full symmetry in the ordering of the protein at the extremum. Evaluating the second derivative mechanical-stability matrix shows $Q_i = Q^\ddagger$ to be an unstable maximum:

$$(\delta^2 F^\ddagger / \delta \epsilon_j \delta \epsilon_i)_{\epsilon_i^*, \epsilon_j^*} = -\delta_{ij} Q^\ddagger (1 - Q^\ddagger) / \lambda^\ddagger T. \quad (8)$$

This is clearly negative, meaning that tuning the energies so that $Q_i = Q^\ddagger$ *maximizes* the free energy at the barrier peak. Since the change in the unfolded state (at $Q \approx 0$) is much weaker than at the

transition state, the barrier height itself is essentially maximized. Substituting eq. (8) into a Taylor expansion of the free energy at the extremum (and using $\lambda^\ddagger = \lambda(Q^\ddagger) \approx 1 - Q^\ddagger$) gives for the rate

$$k = k_{\text{HOMO}} \exp(Q^\ddagger M \overline{\delta \epsilon^2} / 2T^2), \quad (9)$$

which is to be compared with eq. (1) in the supplementary material (obtained by an argument using the random energy model). In terms of the route narrowness measure $\mathcal{R}(Q)$ the change in free energy barrier on perturbation is

$$\delta \Delta F^\ddagger = -(1/2)M\lambda^\ddagger T \mathcal{R}(Q^\ddagger). \quad (10)$$

A variance in contact participations $\overline{\delta Q^2} = 0.05$ which is about 20% of the maximal dispersion ($\approx 1/4$, taking $Q^\ddagger \approx 1/2$) lowers the barrier by about $0.1Nk_B T$ or about $5k_B T$ for a chain of length $N \approx 50$ (believed to model a protein with ~ 100 aa [9]).

We can extend the analysis by perturbing about a structure with mean loop length $\bar{\ell}$, and including effects on the barrier due to dispersion in loop length and correlations between energies and loop lengths. A perturbation expansion of the free energy gives to lowest order:

$$\frac{\delta \Delta F^\ddagger}{M} = -\frac{Q^\ddagger}{2T} \overline{\delta \epsilon^2} - T \frac{9}{8} Q^\ddagger \frac{\overline{\delta \ell^2}}{\bar{\ell}^2} - \frac{3}{4} Q^\ddagger \frac{\overline{\delta \ell \delta \epsilon}}{\bar{\ell}} \quad (11)$$

indicating that the free energy barrier is additionally lowered by structural *variance* in loop lengths, and also when shorter range contacts become stronger energetically ($\delta \ell_i < 0$ and $\delta \epsilon_i < 0$) or longer range contacts become weaker energetically ($\delta \ell_i > 0$ and $\delta \epsilon_i > 0$) i.e. in the model the free energy is additionally lowered when fluctuations are correlated so as to further increase the variance in contact participations. This effect has been seen in experiments by the Serrano group [46, 56].

To test the validity of the theory, we compare the analytical results obtained from our theory with the results from simulation of a 27-mer lattice protein model. The comparison is shown on figure 1 where a full analysis is performed. All energies are in units of the mean native interaction strength $\bar{\epsilon}$.

The rate dependence on heterogeneity should be experimentally testable by measuring the dependencies of folding rate at the transition temperature of a well-designed protein on the *dispersion* of ϕ -values. It is important that before and after the mutation(s) the protein remains fast-folding to the native structure without “off-pathway” intermediates, and that its native state enthalpy remain approximately the same, perhaps by tuning environmental variables.

CONCLUSIONS AND FUTURE WORK. In this paper we have introduced refinement and insight into the funnel picture by considering heterogeneity in the folding of well-designed proteins. We have explored in minimally frustrated sequences how folding is effected by heterogeneity in native contact energies, as well as the entropic heterogeneity inherent in folding to a specific three-dimensional native structure. Specifically we examined the effects on the folding free energy barrier, distribution of participations in the transition state ensemble TSE',¹⁴ as well as the diversity or narrowness of folding routes. For the ensemble of sequences having a given T_F/T_G , homogeneously ordering sequences have the largest folding free energy barrier. For most structures, where topological factors play an important role, this regime is achieved by introducing a large dispersion in the distribution of native contact energies which in practice would be almost impossible to achieve. As we reduce the dispersion in the contact energy distribution to a uniform value $\bar{\epsilon}$, the dispersion of contact participations increases and thus the number of folding routes decreases, the free energy barrier decreases and the total configurational entropy at the TSE' initially increases due to polymer halo effects. The folding temperature is only mildly effected; the prefactor appearing in the rate is probably only mildly effected also, since it is largely a function of T_F/T_G and polymer properties [21]. Tuning the interaction energies further results in more probable contacts having stronger energy. Route diversity decreases to moderate values - there are still many routes to the native state, and T_F/T_G is still sufficiently greater than one. The barrier eventually decreases to zero, at relatively mild dispersion in native contact energy. The funnel picture, with different structural details, is valid for the above wide range of native contact energy distributions. However, tuning the energies further so that probable contacts have even lower energy eventually induces the system to take a single or very few folding routes at the transition temperature. A large dispersion of energies is required to achieve this, and in this regime the folding temperature drops well below the glass temperature range, where folding rates are extremely slow.

Since fine tuning interactions on the funnel may effect the rate, sequences may be designed to fold both faster or slower to the *same* structure of a wild type sequence, depending how the interaction strengths correlate with the entropic likelihood of contact formation. Folding rates in mutant proteins that exceed

those of the wild type have been receiving much interest in recent experiments [46, 56–59]. Enhancement (or suppression) of folding rate to a given structure due to changes in sequence are modeled in our theory through changes in native interactions; our results are fully supported by the experiments cited above. The fact that a minimally frustrated protein is robust to perturbations in the interactions means that at least the folding scenarios depicted in the center 2 rows of fig. 1 are feasible within the ensemble of sequences that fold to the given structure. However the number of sequences should be maximal when all the native interactions are near their average, and the actual width of the native interactions depends on the true potential energy function. Fluctuations in rate due to the weakening or strengthening of non-native traps by sequence perturbations is an interesting topic of future research. The enhancements or reductions in rate we have explored are mild compared to the enhancement by minimal frustration (funneling the landscape): the fine tuning of rates may be a phenomenon manifested by *in vitro* or *in machina* evolution, rather than *in vivo* evolution. Nevertheless rate tuning and folding heterogeneity may become an important factor for larger proteins, where e.g. stabilizing partially native intermediates may increase the overall rate or prevent aggregation. Given that a sequence is minimally frustrated, heterogeneity or broken-ordering-symmetry in fact aids folding, similar to the enhancement of nucleation rates seen in other disordered media [60]. Similar effects have been observed in Monte Carlo simulations of sequence evolution, when the selection criteria involves fast folding rate [33]. Here we see how such phenomena can arise from general considerations of the energy landscape theory. The notion that rates increase with heterogeneity at little expense to native stability contrasts with the view that non-uniform ordering exists merely as a residual signature of incomplete evolution to a uniformly folding state. Adjusting the backbone rigidity or the non-additivity of interactions [10, 61] can also modify the barrier height, possibly as much as the effects we are considering here. There may also be functional reasons for non-uniform folding - malleability or rigidity requirements of the active site may inhibit or enhance its tendency to order. The amount of route narrowness in folding was introduced as a thermodynamic measure through the mean square fluctuations in a local order parameter. The route measure may be useful in quantifying the natural kinetic accessibility of various structures. While structural heterogeneity is essentially always present, the flexibility inherent in the num-

¹⁴We use a prime since we actually look at the barrier peak along the Q coordinate.

ber of letters of the sequence code limits the amount of native energetic heterogeneity possible. However some sequence flexibility is in fact required for funnel topographies [62] and so is probably present at least to a limited degree. We have seen here how a very general theoretical framework can be introduced to explain and understand the effects of local heterogeneity in native stability and structural topology on such quantities as folding rates, transition temperatures, and the degree of routing in the funnel folding mechanism. Such a theory should be a useful guide in interpreting and predicting experimental results on many fast-folding proteins.

We thank Peter Wolynes, Hugh Nymeyer, Cecilia Clementi, and Chinlin Guo for their generous and insightful discussions. This work was initiated while Plotkin was a graduate student with Peter Wolynes. This work was supported by NSF Grant MCB9603839 and NSF Bio-Informatics fellowship DBI9974199.

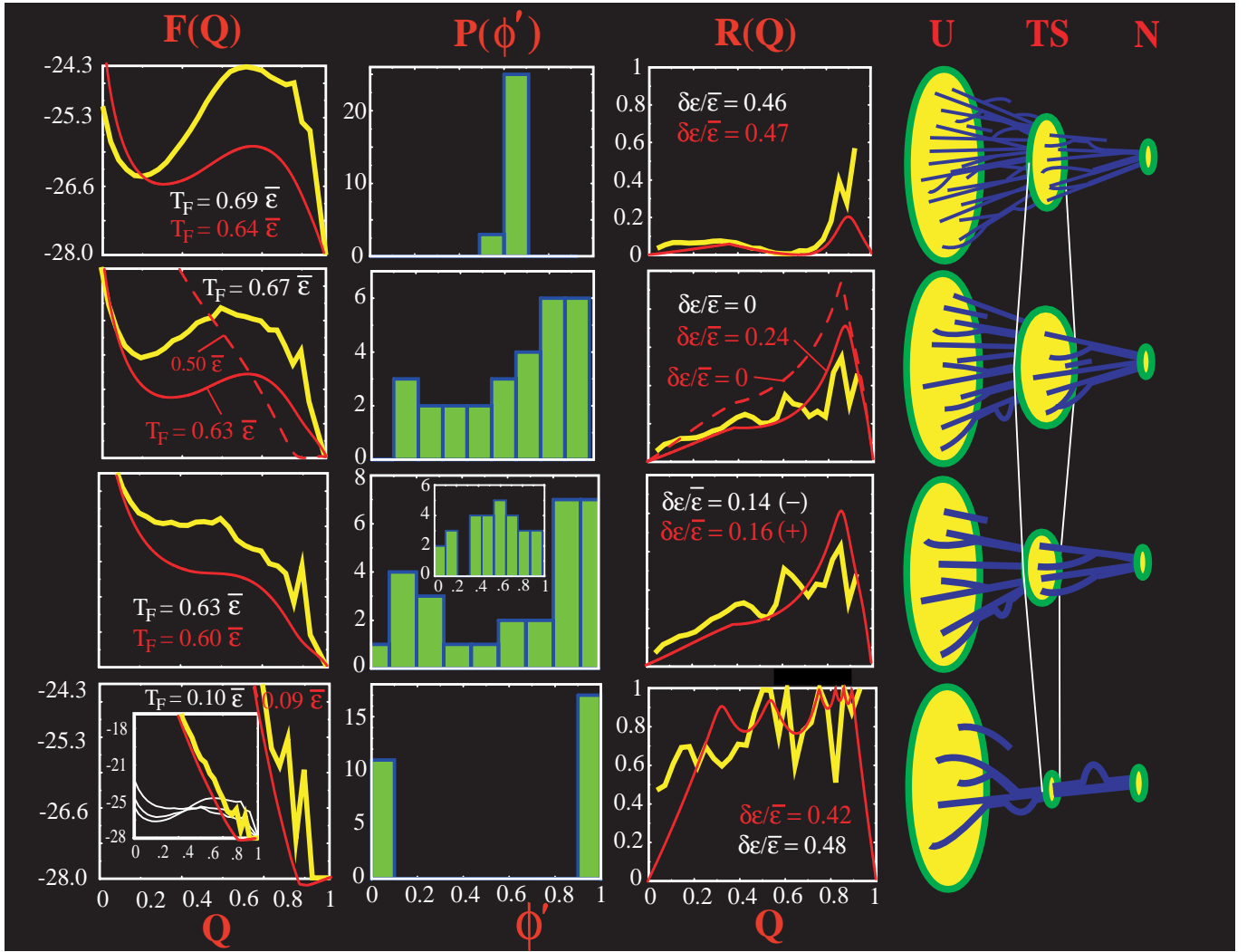


Figure 1:

CAPTION FOR FIG. 1:

The effects of heterogeneity in contact probability (increased from top to bottom) on barrier height F^\ddagger , folding temperature T_F , and ordering heterogeneity are summarized here; plots are for simulations of a 27-mer lattice Gō model (yellow) to the *same* native structure (given in [21]), and for the analytic theory in the text (red). The simulation results make no assumptions on the nature of the configurational entropy; the theoretical results use the approximate state function of eq. (3), along with a cutoff used for the shorter loops so the bond entropy loss for each loop is always ≤ 0 (the same loop length distribution as in the lattice structure is used). In the top row, energies are tuned for both simulation and theory to fully symmetrize the funnel: $Q_i(\epsilon_i^*) = Q$; Second row: energies are then relaxed for the simulation results so they are all equal: $\epsilon_i = \bar{\epsilon}$; energies in the theory are relaxed the same way until a comparable T_F is achieved; Third row: energies are then further tuned to a distribution $\epsilon_i \cong \epsilon_i^o$ that kills the barrier (there are many such distributions - all that is necessary is sufficient contact heterogeneity); The top 3 rows are funneled folding mechanisms with many routes to the native structure. Last row: energies are tuned to induce a single or a few specific routes for folding. All the while the energies are constrained to sum to E_N : $\sum_i \epsilon_i = E_N$. The free energy profile $F(Q)$ (in units of $\bar{\epsilon}$) is plotted in the left column at the folding transition temperature T_F , which is given. The next column shows the distribution of thermodynamic contact probabilities $Q_i(Q^\ddagger) \equiv \phi'$ at the barrier peak (we use the notation ϕ' since this is a thermodynamic rather than kinetic measurement, however for well-designed proteins the two are strongly correlated with coefficient ≈ 0.85 [42]). Only simulation results are shown to keep the figure easy to read; the theory gives ϕ' distributions within $\sim 10\%$ as may be inferred from their similar route measures. The next column shows the route measure $\mathcal{R}(Q)$ of eq. (5) and gives the dispersion in native energies required to induce the scenario of that row ($\mathcal{R}(0, 1) = 0/0$ is undefined and so is omitted from the simulation plots; it is defined in the theory through the limit $Q \rightarrow 0, 1$). The right column shows schematically the different folding routes as heterogeneity is increased; from a maximum number of routes through Q^\ddagger to essentially just one route. **TOP ROW:** In the uniformly ordering funnel we can see first that $P(\phi')$ is a delta function and $\mathcal{R}(Q^\ddagger) = 0$ (c.f. eq. (5)), so ordering at the transition state (or barrier peak Q^\ddagger) is essentially homogeneous. The number of routes through the bottleneck (c.f. eq. (2)) is maximized, as schematically drawn on the right. Branches are drawn in the routes to illustrate the minimum of $\mathcal{R}(Q)$ at Q^\ddagger . The free energy barrier is maximized (eq. (10)), thus the stability of the native state at fixed temperature and native energy is maximized, and so the folding temperature T_F at fixed native energy is maximized. T_F in the simulation is defined as the temperature where the native state ($Q = 1$) is occupied 50% of the time. In the theory, at T_F the probability for $Q \geq 0.8$ is 0.5. A very large dispersion in energies is required to induce this scenario; some contact energies are nearly zero, others are several times stronger than the average. **SECOND ROW:** In the uniform native energy funnel the barrier height is roughly halved while hardly changing T_F , for the following reason. In a Gō model, as the contact energies are relaxed from $\{\epsilon_i^*\}$ to a uniform value $\epsilon_i = \bar{\epsilon}$, the energy of the transition state is essentially constant: initially the energy is $\sum_i Q_i^*(Q^\ddagger) \epsilon_i^* = Q \sum_i \epsilon_i^* = Q E_N$, and as the contact energies are relaxed to a uniform value $\sum_i Q_i \bar{\epsilon} = \bar{\epsilon} \sum_i Q_i = Q E_N$ once again. However the transition state entropy increases and obtains its maximal value when $\epsilon_i = \bar{\epsilon}$, because then all microstates at Q^\ddagger are equally probable since the probability to occupy a microstate is $p_i \sim \exp(-E_i(Q^\ddagger)/T) = \exp(-Q E_N/T)/Z = 1/\Omega(Q^\ddagger)$. The thermal entropy $-\sum_i p_i \log p_i$ then equals the configurational entropy $\log \Omega(Q^\ddagger)$ (its largest possible value). Thus as contact energies are relaxed from ϵ_i^* where they are anti-correlated to their loop lengths (more negative energies tend to be required for longer loops to have equal free energies) to $\bar{\epsilon}$ where they are uncorrelated to their loop lengths, the barrier initially decreases because the total entropy of the bottleneck increases (drawn schematically on the right), i.e. increases in polymer halo entropy are more important than decreases in route entropy. The system is still sufficiently two-state that T_F is hardly changed. $P(\phi')$ is broad indicating inhomogeneity in the transition state, due solely in this scenario to the topology of the native structure since all contacts are equivalent energetically; Routing is more pronounced - when $\epsilon_i = \bar{\epsilon}$, $\mathcal{R}(Q)$ is measure of the intrinsic fluctuations in order due to the natural inhomogeneity present in the native structure; different structures will have different profiles and it will be interesting to see how this measure of structure couples with thermodynamics and kinetics of folding. Loops and dead ends in the schematic drawings are used to illustrate local decreases and increases in $\mathcal{R}(Q)$; these fluctuations are captured by the theory only when the routing becomes pronounced (last row). The solid curves presented for the theory are shown for a reduction in T_F comparable to the simulations. There is still some energetic heterogeneity present as indicated. When

$\epsilon_i = \bar{\epsilon}$ in the theory (dashed curves), the fluctuations in Q_i are somewhat larger than the simulation values, and the entropic heterogeneity is sufficient to kill the barrier- the free energy is downhill at $T_F \cong 0.5\bar{\epsilon}$. The free energy barrier results from a cancellation of large terms and is significantly more sensitive than intensive parameters such as route measure $\mathcal{R}(Q)$. **THIRD ROW:** In approaching the zero-barrier funnel scenario for the simulation, the energies are further perturbed and now begin to anti-correlate with contact probability (and tend to correlate with loop length); i.e. more probable contacts (which tend to have shorter loops) have stronger energies. For the theory not as much heterogeneity is required. Contact energies are still correlated with formation probability as indicated by the signs in parentheses. The free energy barrier continues to decrease until some set of energies $\{\epsilon_i^o\}$ where the barrier at T_F vanishes entirely. All the while the transition temperature T_F decreases only $\sim 10\%$, so that slowing of dynamics (as T_F approaches T_G) would not be a major factor. At this point the ϕ' distribution at the barrier position $Q^\ddagger(\bar{\epsilon})$ is essentially bi-modal, but the distribution at $Q^\ddagger(\{\epsilon_i^o\})$ (inset) is less so because of transition state drift towards lower Q values (the Hammond effect). A relatively small amount of energetic heterogeneity is needed to kill the barrier at T_F . There are still many routes to the native state since $\mathcal{R}(Q^\ddagger) \approx 0.3 - 0.4$, but some contacts are fully formed in the transition state (some $\phi' \cong 1$). **BOTTOM ROW:** As the energies continue to be perturbed to values that cause folding to occur by a single dominant route rather than a funnel mechanism, folding becomes strongly downhill at the transition temperature, which drops more sharply towards T_G : here to induce a single pathway T_F must be decreased to about $1/4$ the putative estimate of T_G (about $T_F(\{\bar{\epsilon}\})/1.6$, see [9]). In this scenario, the actual shape of the free energy profile depends strongly on which route the system is tuned to; Non-native interactions not included here become important. Contact participation at the barrier is essentially one or zero, and the route measure at the barrier is essentially one. The entropy at the bottleneck is relatively small (the halo entropy of a single native core). The energetic heterogeneity necessary to achieve this scenario is again very large - comparable to what is needed to achieve a uniform funnel.

References

- [1] Onuchic, J. N, Luthey-Schulten, Z, & Wolynes, P. G. (1997) *Annu Rev Phys Chem* **48**, 545–600.
- [2] Dill, K. A & Chan, H. S. (1997) *Nat. Struct. Biol.* **4**, 10–19.
- [3] Veitshans, T, Klimov, D, & Thirumalai, D. (1997) *Folding and Design* **2**, 1–22.
- [4] Gruebele, M. (1999) *Annu Rev Phys Chem* **50**, 485–516.
- [5] Bryngelson, J. D & Wolynes, P. G. (1987) *Proc Nat Acad Sci USA* **84**, 7524–7528.
- [6] Goldstein, R. A, Luthey-Schulten, Z. A, & Wolynes, P. G. (1992) *Proc Nat Acad Sci USA* **89**, 4918–4922.
- [7] Shakhnovich, E. I & Gutin, A. M. (1993) *Proc Nat Acad Sci USA* **90**, 7195–7199.
- [8] Leopold, P. E, Montal, M, & Onuchic, J. N. (1992) *Proc Nat Acad Sci USA* **89**, 8721–8725.
- [9] Onuchic, J. N, Wolynes, P. G, Luthey-Schulten, Z, & Socci, N. D. (1995) *Proc Nat Acad Sci USA* **92**, 3626–3630.
- [10] Plotkin, S. S, Wang, J, & Wolynes, P. G. (1997) *J Chem Phys* **106**, 2932–2948.
- [11] Wolynes, P. G. (1996) *Proc Nat Acad Sci USA* **93**, 14249–14255.
- [12] Li, H, Helling, R, Tang, C, & Wingreen, N. (1996) *Science* **273**, 666–669.
- [13] Nelson, E. D, Teneyck, L. F, & Onuchic, J. N. (1997) *Phys Rev Lett* **79**, 3534–3537.
- [14] Wales, D. J & Scheraga, H. A. (1999) *Science* **285**, 1368–1372.
- [15] Ball, K. D, Berry, R. S, Kunz, R. E, Li, F. Y, Proykova, A. A, & Wales, D. J. (1996) *Science* **271**, 963–966.
- [16] Pande, V. S, Grosberg, A. Y, & Tanaka, T. (1995) *J Chem Phys* **103**, 9482–9491.
- [17] Bryngelson, J. D & Wolynes, P. G. (1989) *J Phys Chem* **93**, 6902–6915.
- [18] Bryngelson, J. D, Onuchic, J. N, Socci, N. D, & Wolynes, P. G. (1995) *Proteins* **21**, 167–195.
- [19] Šali, A, Shakhnovich, E, & Karplus, M. (1994) *Nature* **369**, 248–251.
- [20] Boczeko, E. M & Brooks, C. L. (1995) *Science* **269**, 393–396.
- [21] Socci, N. D, Onuchic, J. N, & Wolynes, P. G. (1996) *J Chem Phys* **104**, 5860–5868.
- [22] Lazaridis, T & Karplus, M. (1997) *Science* **278**, 1928–1931.
- [23] Pande, V. S & Rokhsar, D. S. (1999) *Proc Nat Acad Sci USA* **96**, 1273–1278.
- [24] Burton, R. E, Huang, G. S, Daugherty, M. A, Calderone, T, & Oas, T. G. (1997) *Nature Struct Biol* **4**, 305–310.
- [25] Oliveberg, M, Tan, Y, Silow, M, & Fersht, A. (1998) *J Mol Biol* **277**, 933–943.
- [26] Goldbeck, R. A, Thomas, Y. G, Chen, E, Ex-querra, R. M, & Kligar, D. S. (1999) *Proc Nat Acad Sci USA* **96**, 2782–2787.
- [27] Fersht, A. R, Matouschek, A, & Serrano, L. (1992) *J Mol Biol* **224**, 771–782.
- [28] Radford, S. A, Dobson, M, & Evans, P. A. (1992) *Nature* **358**, 302–307.
- [29] Bai, Y, Sosnick, T. R, Mayne, L, & Englander, S. W. (1995) *Science* **269**, 192–197.
- [30] Martinez, J. C, Pisabarro, M. T, & Serrano, L. (1998) *Nature Struct Biol* **5**, 721–729.
- [31] Grantcharova, V. P, Santiago, J. V, Baker, D, & Riddle, D. S. (1998) *Nature Struct Biol* **5**, 714–720.
- [32] Abkevich, V. I, Gutin, A. M, & Shakhnovich, E. I. (1994) *Biochemistry* **33**, 10026–10036.
- [33] Gutin, A. M, Abkevich, V. I, & Shakhnovich, E. I. (1995) *Proc Nat Acad Sci USA* **92**, 1282–1286.
- [34] Panchenko, A. R, Luthey-Schulten, Z, & Wolynes, P. G. (1996) *Proc Nat Acad Sci USA* **93**, 2008–2013.
- [35] Onuchic, J. N, Socci, N. D, Luthey-Schulten, Z, & Wolynes, P. G. (1996) *Folding and Design* **1**, 441–450.
- [36] Shoemaker, B. A, Wang, J, & Wolynes, P. G. (1997) *Proc. Nat. Acad. Sci. USA* **94**, 777–782.

- [37] Portman, J. J, Takada, S, & Wolynes, P. G. (1998) *Phys Rev Lett* **81**, 5237–5240.
- [38] Klimov, D & Thirumalai, D. (1998) *J Mol Biol* **282**, 471–492.
- [39] Sheinerman, F. B & Brooks, C. L. (1998) *Proc Nat Acad Sci USA* **95**, 1562–1567.
- [40] Micheletti, C, Banavar, J. R, Maritan, A, & Seno, F. (1999) *Phys Rev Lett* **82**, 3372–3375.
- [41] Shea, J. E, Onuchic, J. N, & Brooks, C. L. (1999) *Proc Nat Acad Sci USA* **96**, 12512–12517.
- [42] Nymeyer, H, Socci, N. D, & Onuchic, J. N. (2000) *Proc Nat Acad Sci USA* **97**, 634–639.
- [43] Socci, N. D & Onuchic, J. N. (1995) *J Chem Phys* **103**, 4732–4744.
- [44] Abkevich, V. I, Gutin, A. M, & Shakhnovich, E. I. (1995) *J Mol Biol* **252**, 460–471.
- [45] Betancourt, M. R & Onuchic, J. N. (1995) *J Chem Phys* **103**, 773–787.
- [46] Viguera, A. R, Villegas, V, Aviles, F. X, & Serrano, L. (1996) *Folding and Design* **2**, 23–33.
- [47] Plaxco, K. W, Simons, K. T, & Baker, D. (1998) *J Mol Biol* **277**, 985–994.
- [48] Shoemaker, B. A, Wang, J, & Wolynes, P. G. (1999) *J Mol Biol* **287**, 675–694.
- [49] Alm, E & Baker, D. (1999) *Proc Nat Acad Sci USA* **96**, 11305–11310.
- [50] Munoz, V & Eaton, W. A. (1999) *Proc Nat Acad Sci USA* **96**, 11311–11316.
- [51] Anderson, P. W. (1992) *Concepts in solids*. (Addison-Wesley, Reading, Massachusetts).
- [52] Percus, J. K. (1982) in *The liquid state of matter: Fluids, simple and complex*, eds. Montroll, E & Lebowitz, J. (North-Holland, Amsterdam).
- [53] Plotkin, S. S, Wang, J, & Wolynes, P. G. (1996) *Phys Rev E* **53**, 6271–6296.
- [54] Flory, P. J. (1956) *J Am Chem Soc* **78**, 5222–5235.
- [55] Dill, K. A, Fiebig, K. M, & Chan, H. S. (1993) *Proc Nat Acad Sci USA* **90**, 1942–1946.
- [56] Munoz, V & Serrano, L. (1996) *Folding and Design* **1**, R71–R77.
- [57] Hagen, S. J, Hofrichter, J. A, Szabo, A, & Eaton, W. A. (1996) *Proc Nat Acad Sci USA* **93**, 11615–11617.
- [58] Kim, D. E, Gu, H, & Baker, D. (1998) *Proc Nat Acad Sci USA* **95**, 4982–4986.
- [59] Brown, B. M & Sauer, R. T. (1999) *Proc Nat Acad Sci USA* **96**, 1983–1988.
- [60] Karpov, V. G & Oxtoby, D. W. (1996) *Phys Rev B* **54**, 9734–9745.
- [61] Kolinski, A, Godzik, A, & Skolnick, J. (1993) *J Chem Phys* **98**, 7420–7433.
- [62] Wolynes, P. G. (1997) *Nature Struct Biol* **4**, 871–874.